

## Appendix A. Supporting information

### **Machine learning for membrane bioreactor research: principles, methods, applications, and a tutorial**

Yizhe Lai <sup>1</sup>, Kang Xiao <sup>1,2,3,\*</sup>, Yifan He <sup>5</sup>, Xian Liu <sup>3,4</sup>, Jihua Tan <sup>1,3</sup>, Wenchao Xue <sup>5</sup>,  
Aiqian Zhang <sup>3,4</sup>, Xia Huang <sup>6</sup>

<sup>1</sup> Beijing Yanshan Earth Critical Zone National Research Station, College of  
Resources and Environment, University of Chinese Academy of Sciences, Beijing  
101408, China

<sup>2</sup> Key Laboratory of Earth System Numerical Modeling and Application, University of  
Chinese Academy of Sciences, Beijing 101408, China

<sup>3</sup> Environmental Chemistry Faculty, College of Resources and Environment,  
University of Chinese Academy of Sciences, Beijing 101408, China

<sup>4</sup> State Key Laboratory of Environmental Chemistry and Ecotoxicology, Research  
Center for Eco-Environmental Sciences, Chinese Academy of Sciences, Beijing  
100085, China

<sup>5</sup> Department of Energy, Environment, and Climate Change, School of Environment,  
Resources, and Development, Asian Institute of Technology, P.O. Box 4, Klong  
Luang, Pathumthani 12120, Thailand

<sup>6</sup> State Key Joint Laboratory of Environment Simulation and Pollution Control,  
School of Environment, Tsinghua University, Beijing 100084, China

---

\* Corresponding author, E-mail address: [kxiao@ucas.ac.cn](mailto:kxiao@ucas.ac.cn) (K. Xiao)

## Tables

**Table S1.** Summary of common activation functions

**Table S2.** Comparison of decision tree algorithms

**Table S3.** Examples of machine learning models to predict pollutant removal performance in MBRs

**Table S4.** Examples of membrane fouling prediction in MBRs based on support vector machine, decision tree, and ensemble learning models

**Table S5.** Presentation of the virtual raw data for the tutorial example

## Figures

**Figure S1.** Number of publications using machine learning in MBR research

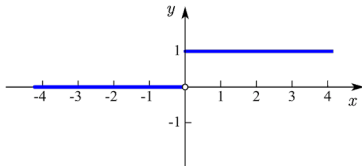
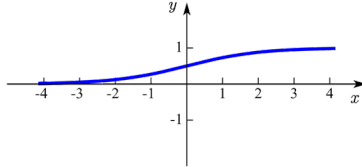
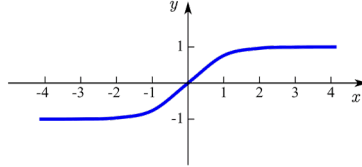
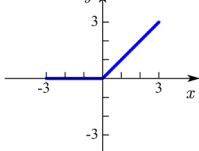
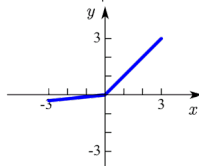
**Figure S2.** Goodness of fit ( $R^2$ ) of ANN models with varied parameters for MBR research: (a) pollutant removal prediction models; (b) fouling prediction models

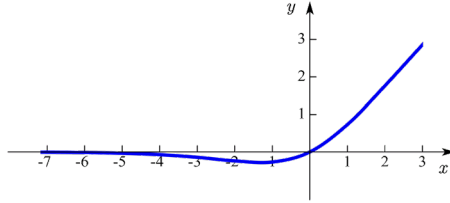
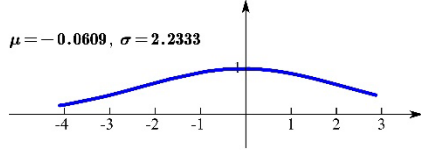
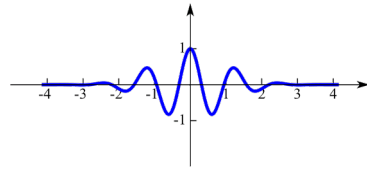
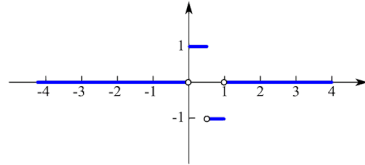
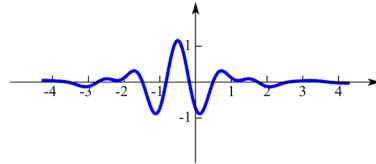
## Notes

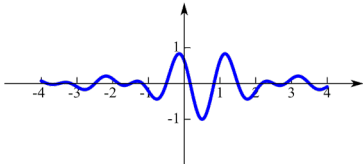
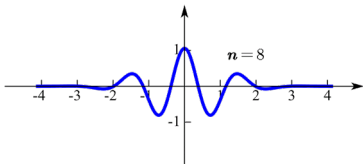
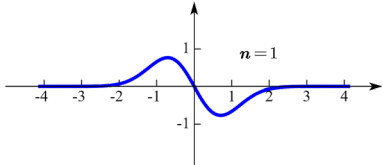
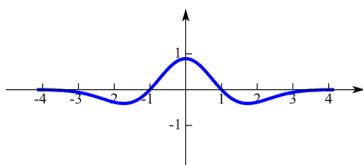
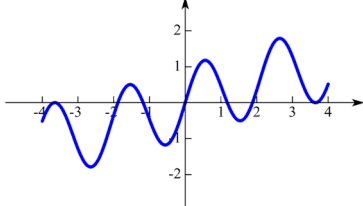
**Section 1.** Set of model parameters

## Tables

**Table S1.** Summary of common activation functions

Model	Activation function	Schematic curve	Feature	Eqn.
MLP	$\text{sgn}(x) = \begin{cases} 0, & x < 0 \\ 1, & x \geq 0 \end{cases}$		<ul style="list-style-type: none"> <li>• Discontinuity with mutation</li> <li>• Not centered on 0</li> </ul>	1
MLP CNN RNN	$\text{sigmoid}(x) = \frac{1}{1 + e^{-x}}$		<ul style="list-style-type: none"> <li>• Insensitive to extreme values</li> <li>• Not centered on 0</li> <li>• Continuous</li> </ul>	2
MLP	$\tanh(x) = \frac{2}{1 + e^{-2x}} - 1$		<ul style="list-style-type: none"> <li>• Insensitive to extreme values</li> <li>• Centered on 0</li> </ul>	3
CNN RNN	$\text{ReLU}(x) = \max(0, x)$		<ul style="list-style-type: none"> <li>• Sensitive to positive values</li> <li>• Insensitive to negative values</li> <li>• Gradient vanishing or gradient explosion</li> </ul>	4
CNN RNN	$\text{LeakyReLU}(x) = \max(\alpha x, x)$ ( $0 < \alpha < 1$ )		<ul style="list-style-type: none"> <li>• Sensitivity to positive values is greater than that to negative values</li> <li>• Increased ReLU range to <math>(-\infty, +\infty)</math></li> </ul>	5

CNN RNN	$\text{Swish}(x) = x \cdot \frac{1}{1 + e^{-x}}$		<ul style="list-style-type: none"> <li>• Sensitive to positive values</li> <li>• Insensitive to minima</li> </ul>	6
RBFNN	$\varphi_{\text{RBF}}(x) = \exp\left(-\frac{\ x - \mu\ ^2}{2\sigma^2}\right)$ where, $\mu$ and $\sigma$ stands for center point and standard deviation, respectively		<ul style="list-style-type: none"> <li>• Symmetry</li> </ul>	7
WNN	$\psi_{\text{Morlet}}(t) = \cos(5t) \exp\left(-\frac{t^2}{2}\right)$		<ul style="list-style-type: none"> <li>• Single frequency sine function</li> <li>• Symmetry</li> </ul>	8
WNN	$\psi_{\text{Haar}}(t) = \begin{cases} 1, & 0 \leq t \leq 0.5 \\ -1, & 0.5 < t \leq 1 \\ 0, & \text{other} \end{cases}$		<ul style="list-style-type: none"> <li>• Compact support</li> <li>• Discontinuity</li> </ul>	9
WNN	$\hat{\psi}_{\text{Meyer}}(t) = \begin{cases} (2\pi)^{-1/2} e^{i\omega/2} \sin[\frac{\pi}{2} v(\frac{3}{2\pi} t -1)], & \frac{2\pi}{3} \leq  t  \leq \frac{4\pi}{3} \\ (2\pi)^{-1/2} e^{i\omega/2} \cos[\frac{\pi}{2} v(\frac{3}{2\pi} t -1)], & \frac{4\pi}{3} \leq  t  \leq \frac{8\pi}{3} \\ 0, & \text{other} \end{cases}$ $v(a) = 35a^4 - 84a^5 + 70a^6 - 20a^7$ where $v(a)$ is the approximate function on $[0,1]$		<ul style="list-style-type: none"> <li>• Non-compact support</li> <li>• Symmetry</li> </ul>	10

WNN	$\psi_{\text{Shannon}}(t) = \frac{\sin \pi(t-1/2) - \sin 2\pi(t-1/2)}{\pi(t-1/2)}$		<ul style="list-style-type: none"> <li>• Non-compact support</li> <li>• Symmetry</li> </ul>	11
WNN	$\psi_{\text{Gaussian}}(t, n) = C_n \cdot \frac{d^n}{dt^n} \exp\left(-\frac{t^2}{2}\right)$ <p>where <math>n = 1, 2, \dots, 8</math>, <math>C_n</math> is a parameter to make the 2-norm of <math>\psi_{\text{Gaussian}}(t, n) = 1</math>;</p> <p>when <math>n=1</math>, <math>\psi_{\text{Gaussian}}(t) = \frac{t}{\sqrt{2\pi}} \exp\left(-\frac{t^2}{2}\right)</math></p>	 	<ul style="list-style-type: none"> <li>• Axial symmetry for even <math>n</math></li> <li>• Central symmetry for odd <math>n</math></li> </ul>	21
WNN	$\psi_{\text{Mexihat}}(t) = c(1-t^2) \exp\left(-\frac{t^2}{2}\right)$ <p>where <math>c = \frac{2}{\sqrt{3}} \pi^{-1/4}</math></p>		<ul style="list-style-type: none"> <li>• Nonorthogonality</li> <li>• Symmetry</li> </ul>	13
WNN	$\psi_{\text{GGW}}(t) = \sin(3t) + \sin(0.3t) + \sin(0.03t)$		<ul style="list-style-type: none"> <li>• Central symmetry</li> </ul>	14

**Table S2.** Comparison of decision tree algorithms

Key point or algorithm name	ID3	C4.5	CART
Feature selection	Information gain, which selects the feature with the greatest information gain	Information gain rate, which selects the feature with the largest information gain ratio	Gini coefficient (Gini), which selects the feature with the smallest Gini coefficient
Record division	Multi-division	Multi-division	Binary division only
Stop splitting conditions	Information gain smaller than the threshold	Information gain ratio smaller than the threshold	Gini coefficient smaller than the threshold, or the number of samples smaller than the threshold
Pruning method	Not supported	Pessimistic error pruning	To minimize the loss function, or use Gini coefficient to measure the loss

**Table S3.** Examples of machine learning models to predict pollutant removal performance in MBRs

Model	Optimization	Hidden layer activation function	Structural features	Input parameter	Output parameter	Training algorithm	Fitting performance	Ref.
WNN			4-9-1	Influent (COD, TN), pH, HRT, F/M	Effluent (COD, TN)		COD: MAPE = 0.041 TN: MAPE = 0.071	Cai et al., 2019b
WNN			4-9-1	Influent (COD, TN), pH, F/M, salinity	Effluent (COD, TN)		COD: MAPE = 0.021 TN: MAPE = 0.038	Cai et al., 2019c
WNN			3-2-1	Influent (COD, NH <sub>3</sub> -N), salinity	Effluent (COD, NH <sub>3</sub> -N)		COD: $R^2 = 0.998$ NH <sub>3</sub> -N: $R^2 = 0.994$	Cai et al., 2019d
MLP		tan-sigmoid	4-3-1	HRT, MLSS, pH, influent COD	Effluent COD	DX	$R^2 = 0.99$ MSE = 0.00147	Cai et al., 2019a
MLP		tan-sigmoid	5-4-1	Influent COD, pH, DO, HRT, COD of MBR	Effluent COD	DX	MSE = 0.008546	Chen et al., 2008
MLP		tan-sigmoid		Influent (COD, NH <sub>3</sub> -N, turbidity, LAS), SRT, HRT, DO, pH	Effluent (COD, NH <sub>3</sub> -N, turbidity, LAS)		COD: MAPE = 0.0514 NH <sub>3</sub> -N: MAPE = 0.0620 turbidity: RMSE = 0.0276 LAS: RMSE = 0.0141	Chen et al., 2009
MLP	GA	tan-sigmoid	4-9-4	$t$ , OLR, Cycle period, TDS	COD, TOC, MLSS, Oil content in sludge	BBP	$R^2 = 0.99$	Pendashteh et al., 2011
MLP		tan-sigmoid	8-(3×3)-4	Influent (COD, NH <sub>3</sub> -N, NO <sub>3</sub> <sup>-</sup> -N, TP), SRT, HRT, Flux, TMP	Effluent (COD, NH <sub>3</sub> -N, NO <sub>3</sub> <sup>-</sup> -N, TP)			Çinar et al., 2006
RBFNN		RBF	5-5-1	Influent (BOD, COD, NH <sub>3</sub> -N, TP), HRT, TDS, MLVSS, pH	Effluent (BOD, COD, NH <sub>3</sub> -N, TP)		$R^2 > 0.99$	Mirbagheri et al., 2015b
MLP		tan-sigmoid	2-(6×20)-1 2-(4×10)-1 2-(4×10)-1 5-(4×10)-1 4-(2×10)-1	pH, EC, Influent (TN, NH <sub>3</sub> -N, TOC, TP, phosphate)	Removal rate of TN, NH <sub>3</sub> -N, TOC, TP and phosphate	LM	TOC: $R^2 = 0.94$ TN: $R^2 = 0.92$ NH <sub>3</sub> -N: $R^2 = 0.92$ TP: $R^2 = 0.77$ phosphate: $R^2 = 0.89$	Viet and Jang, 2021
ML CNN DenseNet		ReLU		$T$ of MBR, $T$ of environment, Flux, influent( $T$ , pH, COD),	Effluent (pH, COD), COD removal rate, Biogas composition, Biogas yield, ORP			Li et al., 2022
LSTM		ReLU		Influent (TOC, TN, TP, COD, NH <sub>3</sub> -N), SS, DO, ORP, MLSS	Removal rate of TN, NH <sub>4</sub> <sup>+</sup> -N, TP		TN: MSE = 0.015 NH <sub>3</sub> -N: MSE = 0.0047 TP: MSE = 0.018	Yaqub et al., 2020
MLP	CV	sigmoid	5-7-1	MLVSS, EC, pH, DO,	Effluent (COD, NH <sub>3</sub> -N,	LM	$R^2 > 0.98$	Giwa et al., 2016

MLP		tan-sigmoid	5-(5×10)-1	Influent (COD, NH <sub>3</sub> -N, phosphate) PAC concentration, pH, Organic properties (conductivity, molecular weight, log K <sub>ow</sub> )	Removal rate of micropollutants	LM	$R^2 = 0.96$	Viet et al., 2022
MLP			5-4-2	HRT, SRT, influent COD, MLSS	Effluent COD, COD removal rate			Ren et al., 2007
MLP		tan-sigmoid	3-15-1	HRT, MLSS, influent COD	COD removal rate	LM	$R^2 = 0.9974$	Banerjee et al., 2022
MLP		sigmoid	5-(2×5)-3	Flux, HRT, reflow ratio, influent (COD, TN, TP)	Effluent (COD, TN, TP)	LM	$R^2 > 0.99$	Almomani, 2020
MLP			5-11-6 5-9-1 5-9-2	Near-infrared spectroscopy	Concentrations of COD, TN, NH <sub>3</sub> -N, NO <sub>3</sub> <sup>-</sup> -N, NO <sub>2</sub> <sup>-</sup> -N, phosphate, SMP, LB-EPS, TB-EPS		$R^2 > 0.97$	Kim et al., 2021b
MLP	CV	log-sigmoid	648-6-1 98-6-1	Two-dimensional fluorescence spectroscopy	Effluent DCE, Concentration of degradation product (Cl <sup>-</sup> , NH <sub>3</sub> )		DCE: $R^2 = 0.863$ Cl <sup>-</sup> : $R^2 = 0.946$ NH <sub>3</sub> : $R^2 = 0.894$	Wolf et al., 2001
MLP	GA	tan-sigmoid	7-9-1	Influent (BOD, COD, TN, TP), SRT, MLSS, Permeability, TMP	Effluent (BOD, COD, TN, TP)	LM	$R^2 > 0.96$	Bagheri et al., 2016
RBFNN	GA	RBF	7-7-1	Influent (BOD, COD, TN, TP), SRT, MLSS, Permeability, TMP	Effluent (BOD, COD, TN, TP)		$R^2 > 0.99$	Bagheri et al., 2016
GBR	CV			DO, MLSS, MLVSS, F/M, reflow ratio, influent (COD, TN)	Effluent (COD, TN, NH <sub>3</sub> -N)		$R^2 = 0.830$	Zhuang et al., 2021

Notes:

EC = electrical conductivity; BBP = batch backpropagation algorithm; DX = gradient descent with momentum and adaptive learning rate backpropagation; GBR = gradient boosting regression; LM = Levenberg-Marquardt; PAC = powdered activated carbon.

The number  $n_1$ -( $n_2$ )- $n_3$  in structural features represents the number of neurons in input, hidden, and output layers, respectively. When  $n_2=n_{2L} \times n_{2N}$ , it represents that the hidden layer has  $n_{2L}$  layers with  $n_{2N}$  neurons per layer. When  $n_2=n_{21}-n_{22}-n_{2i}-\dots-n_{2j}$  (where  $i$  ranges from 1 to  $j$ , and  $j$  represents the number in  $n_2$ ), it represents that the hidden layer has  $j$  layers with  $n_{2i}$  neurons per layer.



**Table S4.** Examples of membrane fouling prediction in MBRs based on support vector machine, decision tree, and ensemble learning models

Model	Optimization	Input parameter	Output parameter	Fitting performance	Ref.
SVM	CV	Aeration volume, TMP	Flux	$R^2 = 0.814$	Yasmin et al., 2017
SVM		MLSS, Temperature, DO, HRT, TMP, Time	Flux	MAPE = 0.0343	Gao et al., 2016
LSSVM		Temperature, Flux, TMP, MLSS	Resistance	$R^2 = 0.99$	Hamed et al., 2019
SVR	Adaptive optimization	Membrane pore size, Aeration volume, Initial flux, TMP, Temperature, Time, MLSS, Sludge particle size	Flux	MSE = 0.06	Gao et al., 2007
SVR		TMP, $\Delta$ TMP, Temperature, MLSS, TP, Phosphate, Kjeldahl nitrogen	TMP	$R^2 > 0.98$	Kaneko and Funatsu, 2013
SVR	CV	HRT, OLR, Temperature, Flux, membrane effective filtration area), influent/effluent water quality (COD, TP, $\text{NH}_3\text{-N}$ , $\text{NO}_3\text{-N}$ ), MLSS, MLVSS, protein and polysaccharide in EPSs	TMP Resistance		Liu et al., 2020
FTSVR		DO, MLSS, pH, Temperature, TMP	Flux	MAE = 0.63 RMSE = 0.7937	Ji et al., 2014
RF		MLSS, TMP, Resistance	Flux	MAPE = 0.046 $R^2 = 0.95$	Li et al., 2020

Note: FTSVR = fuzzy twin support vector regression; LSSVM = least squares support vector machine; PN = protein; PS = polysaccharide

**Table S5.** Presentation of the virtual raw data for the tutorial example

Parameter	Unit	Mean	Standard deviation	Maximum	Minimum
$T$	°C	20.96	1.08	25.25	17.30
MLSS	g/L	10.01	1.00	13.22	6.68
pH	—	7.90	0.12	8.31	7.48
DO	mg/L	2.69	0.18	3.28	2.01
COD	mg/L	501.95	49.94	689.88	323.26
TN	mg/L	28.08	3.03	38.83	19.48
TP	mg/L	4.01	0.39	5.27	2.83
Flux	LMH	17.99	1.02	21.29	15.00
TMP	kPa	18.52	3.44	29.87	6.00

## Figures

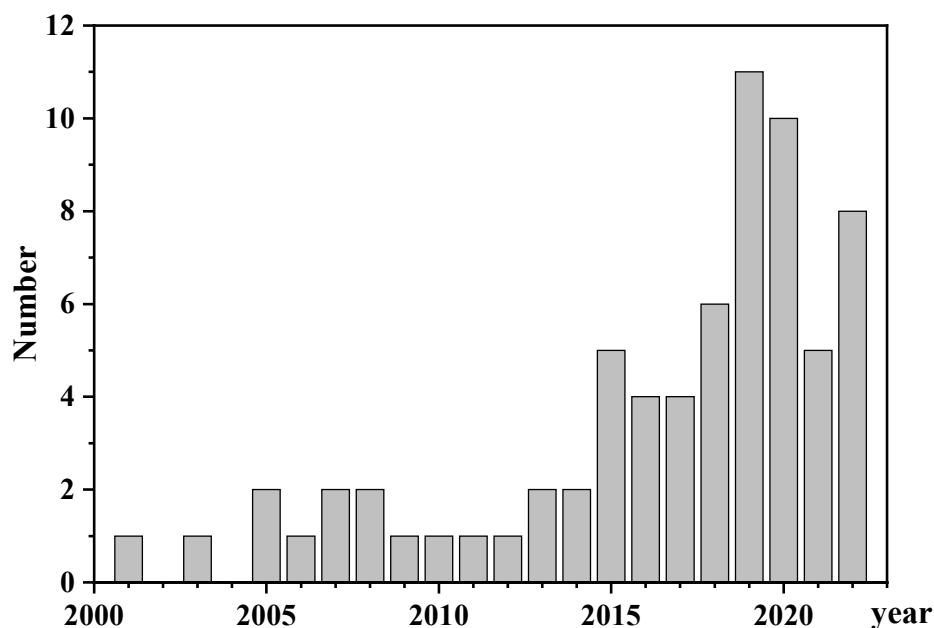


**Figure S1.** Number of publications using machine learning in MBR research

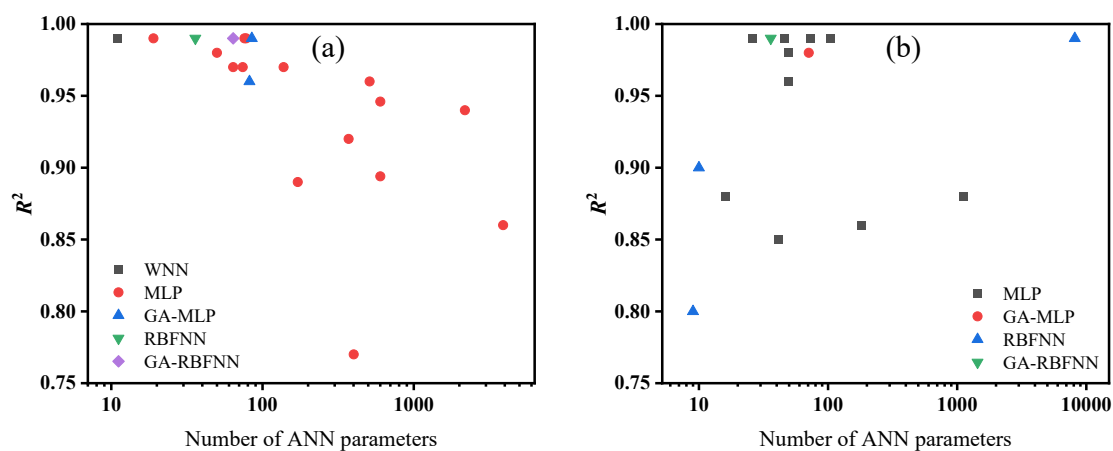


**Figure S2.** Goodness of fit ( $R^2$ ) of ANN models with varied parameters for MBR research: (a) pollutant removal prediction models; (b) fouling prediction models

(Wolf et al., 2001; Aidan et al., 2008; Pendashteh et al., 2011; Mirbagheri et al., 2015a; Mirbagheri et al., 2015b; Bagheri et al., 2016; Giwa et al., 2016; Hazrati et al., 2017; Yasmin et al., 2017; Schmitt et al., 2018; Cai et al., 2019c; Cai et al., 2019d; Chen et al., 2019; Alkmim et al., 2020; Almomani, 2020; Hosseinzadeh et al., 2020; Wahab et al., 2020; Kim et al., 2021a; Viet and Jang, 2021; Banerjee et al., 2022; Irfan et al., 2022; Viet et al., 2022; Yao et al., 2022)

## Notes

### Section 1. Set of model parameters

#### (1) SVM

The *SVMcgForRegress* algorithm was used to optimize the penalty factor  $C$  and the kernel parameter  $G$  for the RBF kernel function. For this tutorial example, the optimal values for  $C$  and  $G$  were 0.5743 and 0.3299, respectively.

#### (2) RF

A larger number of trees were set and the most appropriate number of leaf nodes within the range of {5, 10, 20, 50, 100, 200, 500} was selected based on the MSE parameters. For this tutorial example, the MSE evolution process determined that there were 120 trees, each with 5 leaf nodes. The model was trained using out-of-bag sampling and the influencing factors of membrane fouling formed a high-dimensional data set.

#### (3) BPNN

In this example, the neural network had 8 input neurons and 1 output neuron, corresponding to the number of input and output variables. To establish a single hidden-layer neural network, the number of hidden layer neurons should be between 4 and 14. The number of hidden-layer neurons corresponding to the minimum RMSE was selected for subsequent modeling. According to the RMSE values (Table AD1), the optimal number of hidden-layer neurons was 10, thus the final model topology was set to be 8-10-1 for the BPNN modeling in this example. The neural network toolbox provided with Matlab was used for the modeling, with the activation functions of ‘tansig’ and ‘purelin’ applied to the hidden layer and the output layer, respectively. The LM algorithm was selected for model training, with a maximum number of 1000 iterations, a target error of  $10^{-3}$ , and a learning rate of 0.005.

**Table AD1.** RMSE of the BPNN model with different neurons of hidden layer for the tutorial example

$n$	4	5	6	7	8	9	10	11	12	13	14
RMSE	0.1541	0.0120	0.0275	0.0522	0.0519	0.0354	0.0008	0.0157	0.0466	0.0114	0.0106

#### (4) LSTM

In this example, the neural network had 8 input neurons and 1 output neuron, corresponding to the number of input and output features, respectively. The hidden layer, as composed of LSTM units, was tentatively set to have a total of 24 neurons. The

model training employed a variable learning rate with an initial value of 0.01. After every 125 iterations, the learning rate decayed to 0.2 times of the original. The maximum number of iterations was set to be 500.

#### (5) GA-BP

Based on the BPNN model structure, 8-10-1, the weights and bias of BPNN were further optimized using GA. The GA parameters were set as: the number of population individuals (40), the maximum number of inheritances (50), and the probability of selection, crossover, and mutation operations (0.95, 0.7, and 0.01).

## Reference

- Aidan A, Abdel-Jabbar N, Ibrahim T H, Nenov V, Mjalli F (2008). Neural network modeling and optimization of scheduling backwash for membrane bioreactor. *Clean Technologies and Environmental Policy*, 10(4): 389-395
- Alkmim A R, De Almeida G M, De Carvalho D M, Amaral M C S, Oliveira S (2020). Improving knowledge about permeability in membrane bioreactors through sensitivity analysis using artificial neural networks. *Environmental Technology*, 41(19): 2424-2438
- Almomani F (2020). Prediction the performance of multistage moving bed biological process using artificial neural network (ANN). *Science of the Total Environment*, 744: 140854
- Bagheri M, Mirbagheri S A, Kamarkhani A M, Bagheri Z (2016). Modeling of effluent quality parameters in a submerged membrane bioreactor with simultaneous upward and downward aeration treating municipal wastewater using hybrid models. *Desalination and Water Treatment*, 57(18): 8068-8089
- Banerjee S, Santra B, Kar S, Banerjee D, Ghosh S, Majumdar S (2022). Performance assessment of the indigenous ceramic UF membrane in bioreactor process for highly polluted tannery wastewater treatment. *Environmental Science and Pollution Research*, 29(32): 48620-48637
- Cai Y H, Ben T, Zaidi A A, Shi Y, Zhang K, Lin A Q, Liu C (2019a). Effect of pH on Pollutants Removal of Ship Sewage Treatment in an Innovative Aerobic-Anaerobic Micro-Sludge MBR System. *Water Air and Soil Pollution*, 230(7): 163
- Cai Y H, Li X, Zaidi A A, Shi Y, Zhang K, Feng R Z, Lin A Q, Liu C (2019b). Effect of hydraulic retention time on pollutants removal from real ship sewage treatment via a pilot-scale air-lift multilevel circulation membrane bioreactor. *Chemosphere*, 236: 124338
- Cai Y H, Li X, Zaidi A A, Shi Y, Zhang K, Sun P Q, Lu Z (2019c). Processing Efficiency, Simulation and Enzyme Activities Analysis of an Air-Lift Multilevel Circulation Membrane Bioreactor (AMCMBR) on Marine Domestic Sewage Treatment. *Periodica Polytechnica-Chemical Engineering*, 63(3): 448-458
- Cai Y H, Zaidi A A, Shi Y, Zhang K, Li X, Xiao S H, Lin A Q (2019d). Influence of salinity on the biological treatment of domestic ship sewage using an air-lift multilevel circulation membrane reactor. *Environmental Science and Pollution Research*, 26(36): 37026-37036
- Chen Y, Yu G, Long Y, Teng J, You X, Liao B-Q, Lin H (2019). Application of radial basis function artificial neural network to quantify interfacial energies related to membrane fouling in a membrane bioreactor. *Bioresource Technology*, 293: 122103
- Chen Z, Ren N, Wang A, Zhang Z P, Shi Y (2008). A novel application of TPAD-MBR system to the pilot treatment of chemical synthesis-based pharmaceutical wastewater. *Water Research*, 42(13): 3385-3392
- Chen Z B, Zhou A J, Ren N Q, Tian Y, Hu D X (2009). Pollutants removal and simulation model of combined membrane process for wastewater treatment and reuse in submarine cabin for long voyage. *Journal of Environmental Sciences*, 21(11): 1503-1512
- Çinar Ö, Hasar H, Kinaci C (2006). Modeling of submerged membrane bioreactor treating cheese whey wastewater by artificial neural network. *Journal of Biotechnology*, 123(2): 204-209
- Gao K, Xi X, Wang Z, Ma Y, Chen S, Ye X, Li Y (2016). Use of support vector machine

- model to predict membrane permeate flux. *Desalination and Water Treatment*, 57(36): 16810-16821
- Gao M, Tian J, Li J (2007). The Study of Membrane Fouling Modeling Method Based on Support Vector Machine for Sewage Treatment Membrane Bioreactor, 1393-1398
- Giwa A, Daer S, Ahmed I, Marpu P R, Hasan S W (2016). Experimental investigation and artificial neural networks ANNs modeling of electrically-enhanced membrane bioreactor for wastewater treatment. *Journal of Water Process Engineering*, 11: 88-97
- Hamed H, Ehteshami M, Mirbagheri S A, Zendehboudi S (2019). New deterministic tools to systematically investigate fouling occurrence in membrane bioreactors. *Chemical Engineering Research & Design*, 144: 334-353
- Hazrati H, Moghaddam A H, Rostamizadeh M (2017). The influence of hydraulic retention time on cake layer specifications in the membrane bioreactor: Experimental and artificial neural network modeling. *Journal of Environmental Chemical Engineering*, 5(3): 3005-3013
- Hosseinzadeh A, Zhou J L, Altaee A, Baziar M, Li X (2020). Modeling water flux in osmotic membrane bioreactor by adaptive network-based fuzzy inference system and artificial neural network. *Bioresource Technology*, 310: 123391
- Irfan M, Waqas S, Arshad U, Khan J A, Legutko S, Kruszelnicka I, Ginter-Kramarczyk D, Rahman S, Skrzypczak A (2022). Response Surface Methodology and Artificial Neural Network Modelling of Membrane Rotating Biological Contactors for Wastewater Treatment. *Materials*, 15(5): 1932
- Ji C J, Li C Q, Wang T (2014). The Research of Fuzzy Weighted Twin Support Vector Regression in the MBR Simulation Prediction. Shanghai, China, 3648-3653
- Kaneko H, Funatsu K (2013). A chemometric approach to prediction of transmembrane pressure in membrane bioreactors. *Chemometrics and Intelligent Laboratory Systems*, 126: 30-37
- Kim J H, Shin J K, Lee H, Lee D H, Kang J H, Cho K H, Lee Y G, Chon K, Baek S S, Park Y (2021a). Improving the performance of machine learning models for early warning of harmful algal blooms using an adaptive synthetic sampling method. *Water Research*, 207: 117821
- Kim S Y, Curko J, Kljusuric J G, Matosic M, Crnek V, Lopez-Vazquez C M, Garcia H A, Brdjanovic D, Valinger D (2021b). Use of near-infrared spectroscopy on predicting wastewater constituents to facilitate the operation of a membrane bioreactor. *Chemosphere*, 272: 129899
- Li G Y, Ji J Y, Ni J L, Wang S R, Guo Y T, Hu Y S, Liu S W, Huang S F, Li Y Y (2022). Application of deep learning for predicting the treatment performance of real municipal wastewater based on one-year operation of two anaerobic membrane bioreactors. *Science of the Total Environment*, 813: 151920
- Li W W, Li C Q, Wang T (2020). Application of machine learning algorithms in MBR simulation under big data platform. *Water Practice and Technology*, 15(4): 1238-1247
- Liu J, Kang X, Luan X, Gao L, Tian H, Liu X (2020). Performance and membrane fouling behaviors analysis with SVR-LibSVM model in a submerged anaerobic membrane bioreactor treating low-strength domestic sewage. *Environmental Technology & Innovation*, 19: 100844
- Mirbagheri S A, Bagheri M, Bagheri Z, Kamarkhani A M (2015a). Evaluation and prediction of membrane fouling in a submerged membrane bioreactor with simultaneous upward and downward aeration using artificial neural network-

- genetic algorithm. *Process Safety and Environmental Protection*, 96: 111-124
- Mirbagheri S A, Bagheri M, Boudaghpour S, Ehteshami M, Bagheri Z (2015b). Performance evaluation and modeling of a submerged membrane bioreactor treating combined municipal and industrial wastewater using radial basis function artificial neural networks. *Journal of Environmental Health Science and Engineering*, 13: 17
- Pendashteh A R, Fakhru'l-Razi A, Chaibakhsh N, Abdullah L C, Madaeni S S, Abidin Z Z (2011). Modeling of membrane bioreactor treating hypersaline oily wastewater by artificial neural network. *Journal of Hazardous Materials*, 192(2): 568-575
- Ren N Q, Yan X F, Chen Z B, Hu D X, Gong M L, Guo W Q (2007). Feasibility and simulation model of a pilot scale membrane bioreactor for wastewater treatment and reuse from Chinese traditional medicine. *Journal of Environmental Sciences*, 19(2): 129-134
- Schmitt F, Banu R, Yeom I T, Do K U (2018). Development of artificial neural networks to predict membrane fouling in an anoxic-aerobic membrane bioreactor treating domestic wastewater. *Biochemical Engineering Journal*, 133: 47-58
- Viet N D, Jang A (2021). Development of artificial intelligence-based models for the prediction of filtration performance and membrane fouling in an osmotic membrane bioreactor. *Journal of Environmental Chemical Engineering*, 9(4): 105337
- Viet N D, Lee H, Im S J, Jang A (2022). Fate, elimination, and simulation of low-molecular-weight micropollutants in an integrated activated carbon-fertiliser drawn osmotic membrane bioreactor. *Bioresource Technology*, 351: 126972
- Wahab N A, Mahmod N, Vilanova R (2020). Permeate Flux Control in SMBR System by Using Neural Network Internal Model Control. *Processes*, 8(12): 1672
- Wolf G, Almeida J S, Pinheiro C, Correia V, Rodrigues C, Reis M a M, Crespo J G (2001). Two-dimensional fluorometry coupled with artificial neural networks: A novel method for on-line monitoring of complex biological processes. *Biotechnology and Bioengineering*, 72(3): 297-306
- Yao J Q, Wu Z Y, Liu Y, Zheng X Y, Zhang H B, Dong R J, Qiao W (2022). Predicting membrane fouling in a high solid AnMBR treating OFMSW leachate through a genetic algorithm and the optimization of a BP neural network model. *Journal of Environmental Management*, 307: 114585
- Yaqub M, Asif H, Kim S, Lee W (2020). Modeling of a full-scale sewage treatment plant to predict the nutrient removal efficiency using a long short-term memory (LSTM) neural network. *Journal of Water Process Engineering*, 37: 101388
- Yasmin N S A, Wahab N A, Yusuf Z (2017). Modeling of Membrane Bioreactor of Wastewater Treatment Using Support Vector Machine. Melaka, MALAYSIA: Springer, Singapore, 485-495
- Zhuang L P, Tang B, Bin L Y, Li P, Huang S S, Fu F L (2021). Performance prediction of an internal-circulation membrane bioreactor based on models comparison and data features analysis. *Biochemical Engineering Journal*, 166: 107850